Tribological investigation of a greased contact subjected to contact dynamic instability

Ilaria Ghezzi, Davide Tonazzi, Michael Rovere, Cédric Le Coeur, Yves Berthier, Francesco Massi

Tribological investigation of a greased contact subjected to contact dynamic instability

Ilaria Ghezzi [1,2,3], Davide Tonazzi [1], Michael Rovere [3], Cédric Le Coeur [3], Yves Berthier [2], Francesco Massi [1]

1. DIMA, University La Sapienza of Rome, Via Eudossiana 18,00184 Rome, Italy.

2. INSA-Lyon, CNRS UMR5259, LaMCoS, F-69621, Bâtiment S. Germain, Avenue Jean Capelle O, 69100 Villeurbanne, France.

3. SOMFY S.A., R&D Center, 50 Avenue du Nouveau Monde, 74300 Cluses, France

KEYWORDS

Friction Induced Vibrations; Stick-slip; lubricated contact; dynamic instabilities

Abstract

A systematic approach to the stick-slip problem of a greased contact is proposed, combining experimental tribological analyses with numerical dynamic simulations. Considering the specific application case of a mechanical spring-brake, the lubricated contact is here analysed. The stick-slip instability on such contact is the result of the coupling between the brake dynamics and the frictional response of the greased contact. The local frictional response has been characterized by experimental tests carried out on a tribometer, reproducing as close as possible the operating parameters. The contact conditions bringing to stick-slip instability are then investigated. The local frictional response is coupled with the system dynamics by using lumped numerical model, in order to better evaluate the unstable dynamic response of the system.

1. Introduction

Considering mechanical systems in relative motion with a frictional interface, during the sliding of one body over another, friction-induced instabilities and stick-slip motion can occur [1–4]. In this case, the relative motion is not continuous but characterized by a series of "sticks" and "slips" [5]. These forms of vibration are often undesirable and can cause excessive wear of components, surface damage [6, 7], fatigue failure, and fastidious noise [2, 3]. The problem becomes even more complicated when a lubricated contact is involved.

In different mechanical systems the lubrication of the surfaces in contact and in relative motion is often used to reduce the friction and to prevent the wear of the materials in contact [5, 7–9]. However the lubrication can play also a key role in the contact instabilities, going to worsen and aggravate the friction-induced vibrations appearance [10]. The presence of self-excited vibrations caused by friction can seriously degrade the nominal operating conditions,

including the lubricant performances. Nevertheless, nowadays, in literature few works deal with stick-slip instability in lubricated systems [10–15].

The presence of friction-induced vibrations are mainly due to a combination of forcing or self-excited nonlinear oscillations of the mechanical system in the presence of friction forces [2, 16–18]. The coupling between the friction force variation and the resulting motion induces a loss of stability of the equilibrium state, which can lead to self-excited oscillations [13]. A relevant number of works has been dedicated to investigate different possible mechanisms at the origins of dynamic instabilities occurring in sliding contact: sprag-slip [19, 20], mode lock-in [21, 22], negative slope of friction coefficient [23], etc. In all this cases, the system dynamics is unstable and is excited by the contact forces. In particular, the sudden change of the sliding speed of the bodies in contact, resulting in a jerking motion of the frictional bodies, is the so called stick-slip effect [3, 23–25].

Strong vibrations of the system are induced by impulsive excitations due to the sudden drops of the tangential force along the motion [1]. In order to explain the phenomenon an idealized physical system consisting of a mass-spring-damper sliding on a moving belt has been considered very often [26]. The macroscopic intermittent motion has been attributed to different causes. The most widely accepted cause for stick-slip is that the static friction coefficient (μ_s) is markedly greater than the kinetic friction coefficient (μ_k) or, more rigorously, that μ_k drops rapidly at small speeds [3, 27]. Also a coupling between the normal and tangential motion can bring to dynamic instabilities, even if the friction coefficient is maintained constant and no difference between the kinetic and the static friction is accounted for [28, 29]. As well, analyses of the fast dynamics of the interface and wave propagation at the interface showed the occurrence of stick-slip in frictional system with constant friction coefficient, where the local relative compliance of the interfaces dominate the stick-slip occurrence [30–32]. Nevertheless, even if not necessary, the negative friction-velocity slope and the difference between static and dynamic friction coefficient increase the propensity to stick-slip, by destabilizing the system dynamics.

Several contact parameters can affect the response of a frictional system, such as normal load [3, 28, 33], sliding velocity [34–36], surface roughness [29, 37], component geometries [21], material properties [22, 38–40], etc. Any change of one contact parameter can interact with the other ones, affecting the contact dynamics and therefore the frictional and vibrational response of the system. For these reasons, dealing with stick-slip on a real brake system, where the parameters are difficult to be controlled and separated, results to be extremely tricky.

Moreover, the presence of lubrication makes the phenomenon extremely interesting and complex from a tribological and vibrational point of view. The presence of a lubricant layer between the contact surfaces affects the frictional response. The friction force and the sliding velocity are linked by the formation of a fluid interface [13]. The lubrication regimes (boundary, mixed, elasto-hydrodynamic and hydrodynamic regime) are non-linear function of the contact load, the lubricant viscosity and velocity [41, 42]. Furthermore, the frictional response of the lubricant layer confined between the two shearing surfaces will depend on the operating conditions (contact pressure, sliding velocity and temperature) [10].

It is therefore clear that the stick-slip in lubricated contact is a complex phenomenon. The key to its understanding is the taking into account of both the local behaviour of the lubricated contact and the dynamic response of the entire system.

The understanding of frictional instabilities in lubricated contacts represent an interesting challenge, from both a scientific and industrial point of view [10]. The present work proposes a systematic approach to the stick-slip problem of a lubricated contact. First the focus is on the analysis of the local frictional contact response, in order to evaluate the friction coefficient curves as a function of the imposed boundary conditions, through experimental tests on a dedicated tribometer. Then, the obtained information will be integrated in a lumped numerical model to evaluate the unstable dynamic response of the entire system (i.e. the stick-slip phenomena) and identify the parameters that most influence its appearance. The present work is focused on a real industrial case in order to deploy the results obtained in a more realistic and detailed manner. The investigated subject is a mechanical brake used in tubular electric actuators [43–45], which can generate frictional instabilities in the grease lubricated contact between the two main brake components.

The paper is organized as follows. Section 2 describes the mechanical brake system object of the study, the lubricated contact bodies in sliding being investigated, the test bench and the protocol used to reproduce the real contact conditions. Section 3 presents the frictional response at the contact, as function of the different investigated boundary conditions. Section 4 is an explanation of the lumped model representing the entire system (i.e. the electic tubular actuator) and a discussion about the preliminary results obtained. Finally, the conclusions follow in Section 5.

2. Stick-slip occurrence in spring brake systems

The mechanical spring-brake system located in an electric tubular actuator is here investigated as example for the application of the analysis of the stick-slip phenomenon and its appearance in greased contacts. The actuator in Figure 1 [43, 44] is composed by an electric motor (A) and a gearbox (B), in which a mechanical spring brake (C) is included. Such a system has to raise and lower the output load.

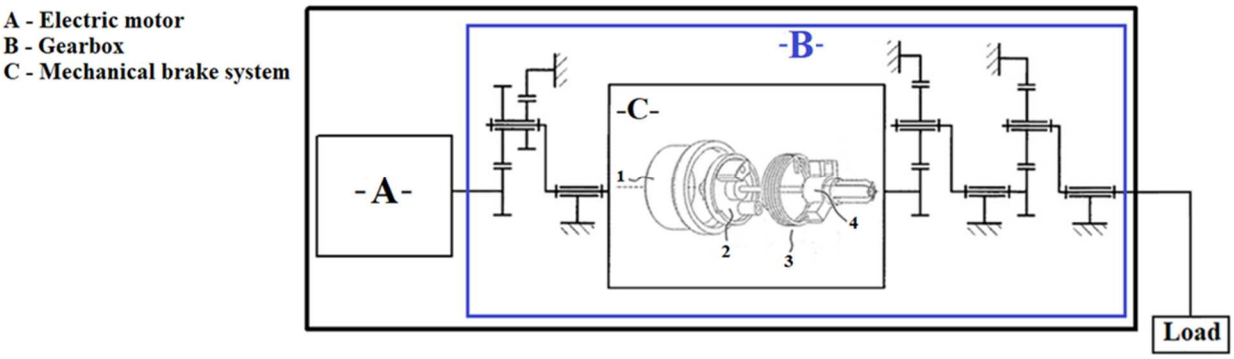

Figure 1: Scheme of the electric tubular actuator object of study.

The spring brake concept is manly composed by four different parts [44]: the drum (1), the torsional spring (3), the driver (2) and the side frame (4). Aim of the brake system is to braking and support the load, by proving a braking torque. The external drum is fixed and the torsional spring is tightened inside it. The contact interface, between the outer surface of the spring and the inner surface of the drum, is lubricated with a synthetic commercial grease. The driver (2) is stuck inside the drum and is directly connected to the engine, allowing the transmission of the rotation to the spring. The side frame (4), connected to the other end of the spring, supports the output load. During the load descent phase, the widening of the spring assures the braking, thanks to the increase of the contact pressure (and of the resulting frictional force) at the lubricated contact between the fixed cylinder and torsional spring. A uniform film of grease is used in the contact area to decrease wear and stabilize the friction between the components.

During the descent phase, the operating conditions can induce a contact instability at the greased contact between the spring and the fixed cylinder. The presence of the stick-slip phenomena was detected with brakes of different sizes, materials, geometries of the spring coil, rotational speed and output load.

Figure 2 shows the time signals and the respective spectrograms of the acceleration measured on the external surface of the actuator, during the descent phase at ambient temperature (25°) and higher temperature (80°) respectively.

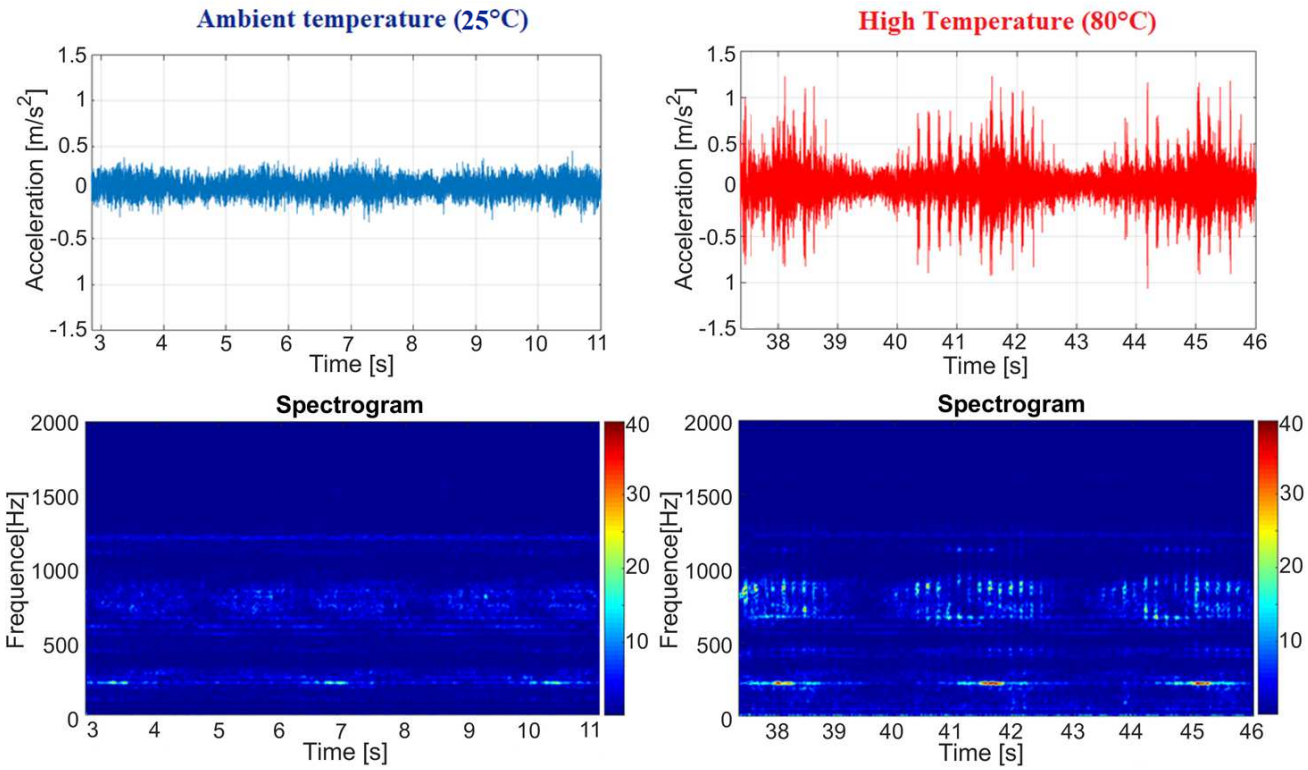

Figure 2: Time signals and the respective spectrograms of the acceleration, during the descent phase at ambient temperature, 25°C (blue signal), and higher temperature, 80°C (red signal).

A typical stick-slip impulsive responses can be observed at high temperature (red curve), after some completed cycles of the load (i.e. ascent and descent phases), when the temperature at the contact increase.

A discontinuous motion characterized by alternating phases of sliding and sticking of the spring on the cylinder occurs inducing an impulsive vibrational response of the contact bodies, exciting the entire structure. The unstable frictional response of the system can be a consequence of the frictional contact behaviour and its interaction with the system dynamics. In fact, the interaction of the local contact response and the dynamics of the whole frictional system is at the origins of the stick-slip occurrence [2]. For this reason, an investigation of the local frictional response of the greased contact, under both ambient and high temperature, is needed to understand the local conditions that can bring to the dynamic instability.

3. Frictional analysis of the local greased contact

The local contact response is here investigated through simplified tests, using a dedicated tribometer (*TriboAir* tests bench [29, 38, 46]) properly adapted to the case study. The setup allows for reproducing and measuring the frictional response during the imposed relative motion between two bodies, under well controlled boundary conditions [29].
A simplified tribological system has been developed to measure the local frictional response of the contact, taking into account the real case study (Figure 3).

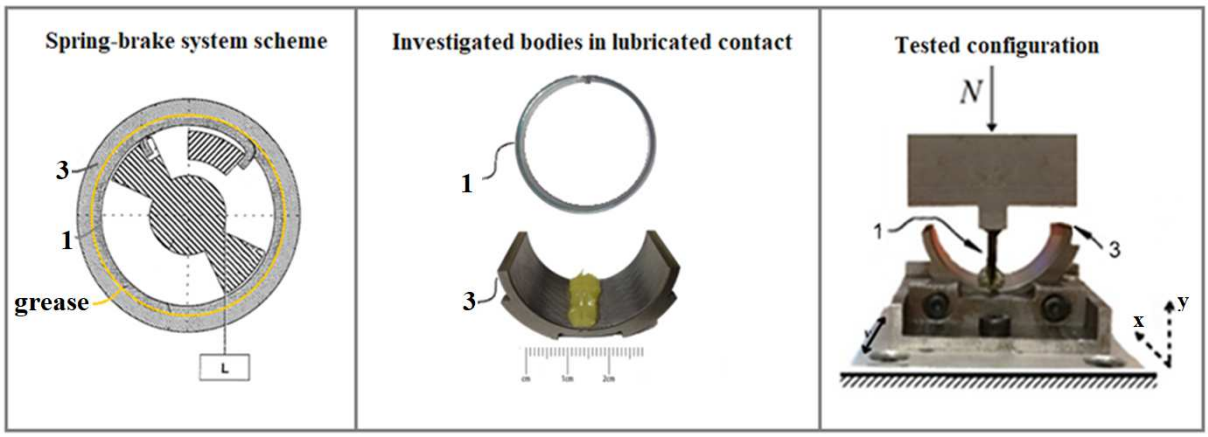

Figure 3: From the spring brake system (left), to the tested tribological system (right). (1) Torsional spring; (3) brake drum.

A spring spire, obtained from the brake spring, is rigidly linked to a dedicated holder; the spring is put in contact with the drum and then a relative motion along the tangential direction (x-axis) is imposed to the system. The brake components are directly cut from the real ones, used in the investigated spring brake systems, to maintain as much as possible the same material and surface features.
The two contact surfaces at the beginning of each test are lubricated with a homogeneous film of complex lithium grease, used in the real brake system.
Using the tribometer shown in Figure 4, a normal load (N) is imposed and the two surfaces are rubbed against each other along the tangential direction at controlled speed (v).
The relative movement of the sample is allowed by an air bearing system (a1), coupled with a linear voice coil (b) (BEI KIMCO LA30-75-001A), assuring the absence of unwanted source of parasitic vibrations, which could negatively affect the measures.

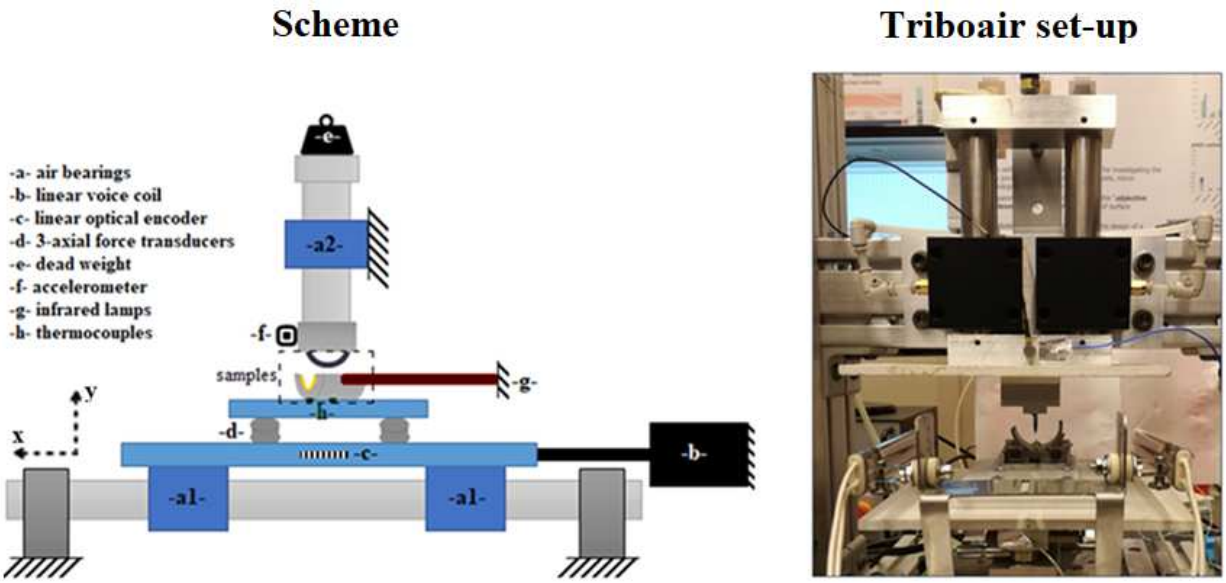

Figure 4: TriboAir test bench (right figure) and its operating scheme (left side). (-b-) identify the linear voice coil, (-a1- and -a2-) the air bearings systems, (-e-) the loading system, (-c-) the linear encoder, (-d-) the 3-axial force transducers, (-f-) the accelerometer and (-g-) the infrared emitters.

The linear voice coil (b) allows for a planar controlled movement of the base. The velocity and position of the voice coil is determined by a controller (ELMO Gold DC Whistle) and a linear optical encoder (c), which closes the position command loop. Two 3-axial force transducers (d) (Kistler 9017B) are mounted on the translating base of the test bench, in order to measure the overall normal and tangential contact forces [29]. Other two air bushings (a2) hold the upper sample and allow for the application of the load, by dead weights (e), along the normal direction with respect to the contact. An accelerometer (-f-) is used for monitoring the vibrational response of the system during the frictional tests.
In order to perform tests at different temperatures, two infrared (IR) emitters (-g-) are placed on the sides of the samples in contact, and two thermocouples (-h-) are used for monitoring the temperature of the samples as close as possible to the contact interface. Two ceramic plates are used to protect sensitive test-bench parts from overheating.
The tangential and normal force, the acceleration and the temperature signals are acquired by an 8-channels acquisition-card (NI 4472) with a sampling frequency of 5120 Hz and then post-processed by Matlab ©.

3.1.Reproduction of the contact conditions

The experimental test bench has been designed and developed to measure the contact frictional behavior under well controlled boundary conditions. The tests have been performed to characterize the local frictional response, by identifying the evolution of the friction coefficient as a function of speed, temperature and contact pressure. Before starting the experimental campaign, the values and the ranges of the controlled boundary conditions (sliding velocity, temperature and contact pressure) were selected to be representative, as much as possible, of the operative conditions in the real brake system. All the tests were performed with well-defined imposed conditions:

- The relative displacement between the drum and the spring spire is characterized by a sliding distance of 10 mm. A complete cycle consists of a back and forward of the spring spire that moves on the surface of the drum.
- The samples were tested imposing a constant sliding velocity of the drum. The velocity range (from 0.1 to 20 mm/s) was selected in order to analyse the dynamic friction coefficient in different operating regimes of lubrication and to evaluate the contact behaviour in function of the sliding velocity. The acceleration is properly selected in order to have a short linear increase and decrease of the velocity, with a plateau at the maximum sliding speed along the 10mm of distance.
- The spring brake systems are characterized by a variable contact pressure; during the braking, the rotating torsional spring undergoes a contact pressure range depending on the position of the descending load and on the angular sector of the contact between the drum and the spring. In this regards, a wide range of normal loads, covering the expected range of contact pressure, was chosen (from 5 to 50N). Passing from the lower to the highest imposed normal load it is possible to analyse the friction coefficient as a function of the load (pressure).
- In order to investigate the influence of the grease response as a function of the temperature, two different temperature conditions were imposed during the tests, i.e. ambient temperature (25 °C) and high temperature (80 °C). Two infrared emitters have been used to heat gradually the system up to the wished temperature (80°C) in order to have a homogeneous heating of the contact materials (spring spire and drum).

Every condition is tested for 4 cycles. Moreover, at the end of each set of tests as a function of the speed, the first test condition is repeated in order to verify the repeatability of the contact conditions at the interface. An example of the applied protocol is show in Table 1.

Tests number	**Sliding velocity *v* [mm/s]**	**Normal Load *N* [N]**	**Temperature [°C]**
1	0.1	20	25
2	1	20	25
3	5	20	25
4	10	20	25
5	20	20	25
1*	0.1	20	25
6	0.1	20	80
7	1	20	80
8	5	20	80
9	10	20	80
10	20	20	80
6*	0.1	20	80
1**	0.1	20	25

Table 1: Example of a test protocol with constant load equal to 20N, variable velocity and temperature, in order to evaluate the local lubricated contact response.

For each tests, the friction coefficient is calculated as the ratio between the tangential force and the imposed normal force, acquired through the force transducers (Figure 4 -d-).
As shown in the Table 1, the test number 1 is repeated after the test number 6. Then the system is heated gradually reaching the temperature of 80°C and the tests are repeated with the same conditions, maintaining the temperature constant. After the test number 6*, the solids in contact are left cooling down until the ambient temperature is reached. Then, the tests number 1 is repeated again (number 1** in the Table 1). The same protocol in the same conditions is used to tests the others imposed normal loads.

3.2.Local frictional response of the greased contact

The experimental tests on the simplified contact configuration allow for characterizing the local frictional response of the greased contact between the spring and the drum surfaces. The normalized friction coefficient is calculated for each test as the ratio between tangential and normal force, acquired through the tri-axial force transducers (Figure 4 -d-), and then normalized to the maximum value obtained for all the test campaign.
As an example, Figure 5 shows the acquired signals for the test at 0.1 mm/s, 20 N of normal load and 25 °C (test number 1 – Table 1), during two cycles of oscillation.

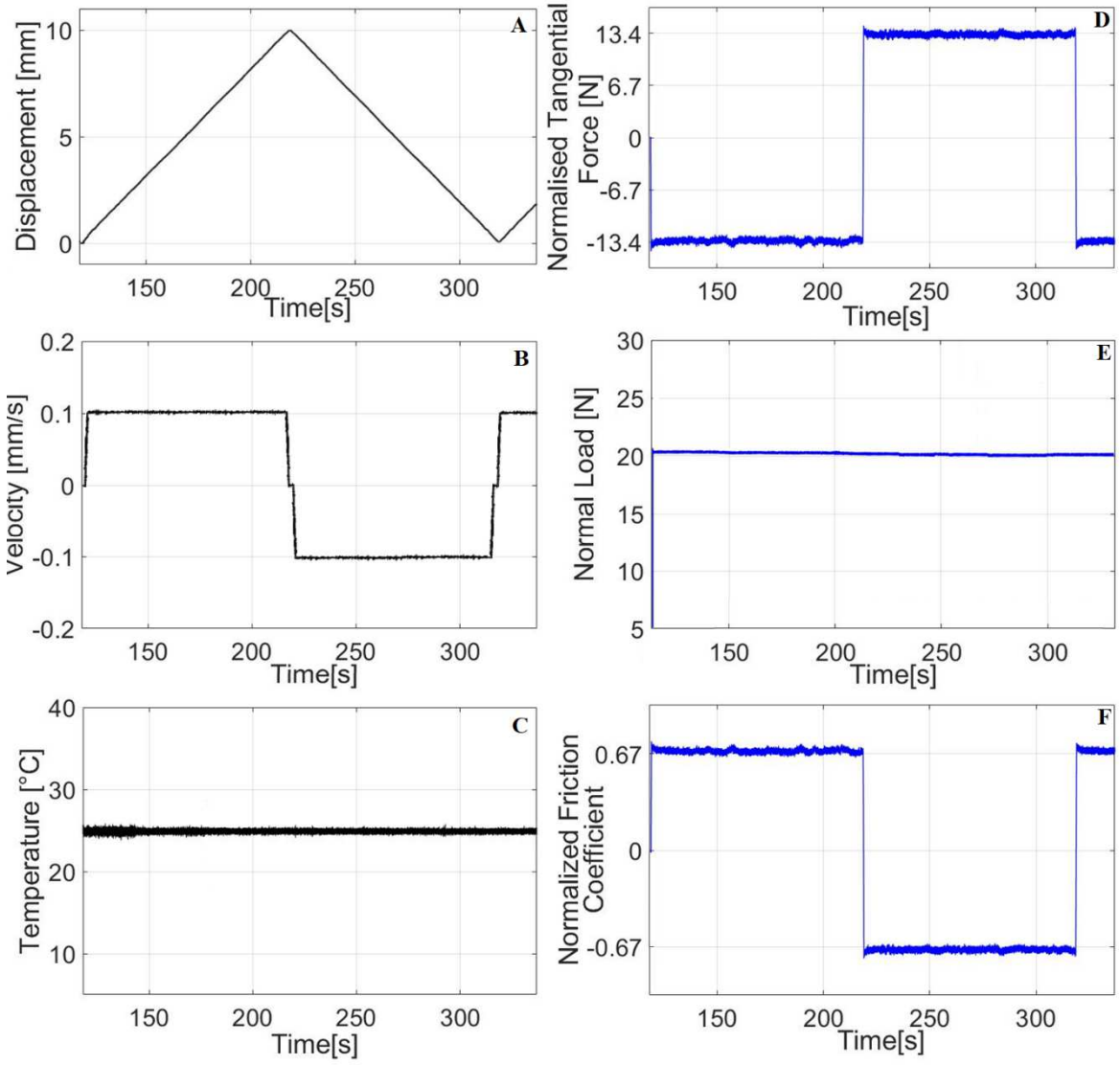

Figure 5: Acquired signal of the test number 1 (sliding velocity 0.1mm/s, imposed normal load 20N and ambient temperature, 25°C). A - displacement of the drum, B - sliding velocity of the drum, C - temperature of the contact interface, D - Normalized Friction Force, E - Imposed Normal Load, F - Normalized Coefficient of Friction, all in function of time [s].

From the up to the bottom, the following signals are displayed: imposed displacement, sliding velocity and temperature of the drum on the left, the normalized tangential force, the imposed normal load and the normalized coefficient of friction on the right (Figure 5).
Figure 6 shows the time evolution of the normalized friction coefficient, for the same velocity and load conditions, but at respectively 25 °C (blue curve) and 80 °C (red curve).

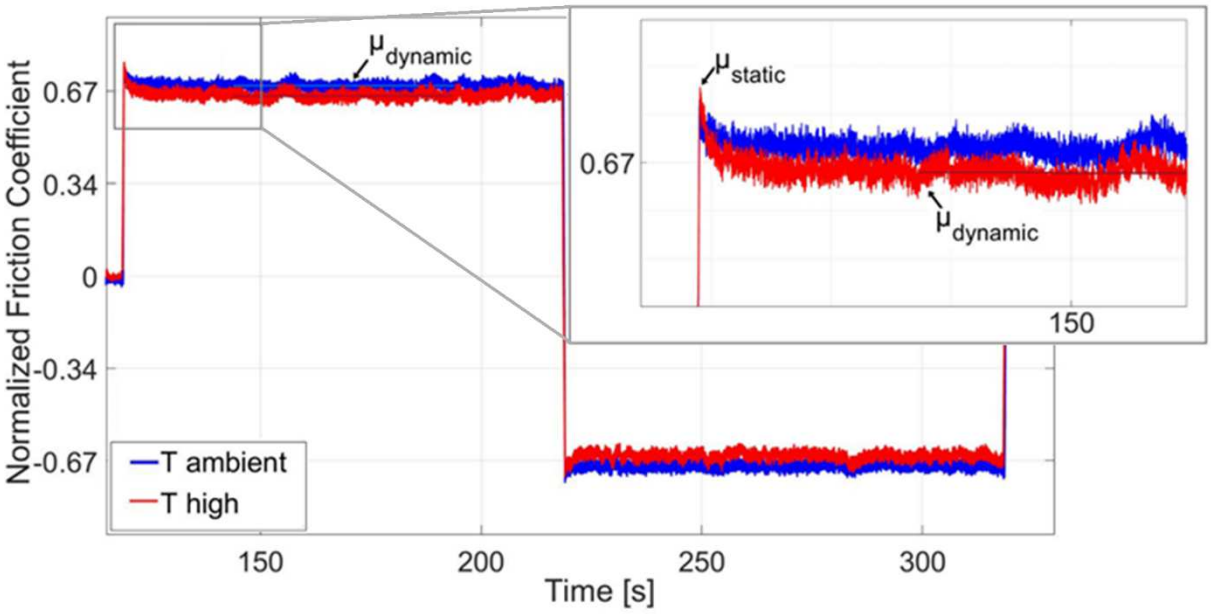

Figure 6: Time evolution of the normalized friction coefficient, for the same velocity and load conditions, but at respectively 25 °C (blue curve) and 80 °C (red curve). Difference between the μ_{static} and $\mu_{dynamic}$ at ambient and high temperature condition is highlighted in the zoom.

It is possible to appreciate the trend of the friction coefficient during a single cycle (i.e. a single roundtrip of the spring spires on the greased drum). The normalized dynamic friction coefficient (μ_d) is calculated as the average value of the curve when the imposed relative speed is constant.
From the test performed at lowest velocity (0.1 mm/s), where the inertia contribution to the tangential force is negligible, it's possible to extract the static friction coefficient just before the sliding occurs. The peak of the friction coefficient (μ_s) at the starting of the motion, in Figure 6, represents the frictional resistance at the first detachment between the two surfaces in contact. Comparing the same tests performed with the two different temperature conditions, maintaining unchanged the other boundary conditions, it is possible to observe a lowering of the dynamic friction coefficient with the increasing of the temperature.
On the contrary, the static friction coefficient is slightly increased at higher temperature. Consequently, the difference between static and dynamic friction coefficients ($\mu_s - \mu_d$) is larger at higher temperature (80 °C).
Figure 7 shows the static and dynamic friction coefficients, calculated at the different sliding speeds for the tested normal loads. The evolution of the friction coefficient with the velocity is characterized by a high static friction coefficient, followed by a sudden drop of the friction coefficient calculated at 0.1mm/s and a following increase with the velocity, until reaching a stabilized value at about 10mm/s.

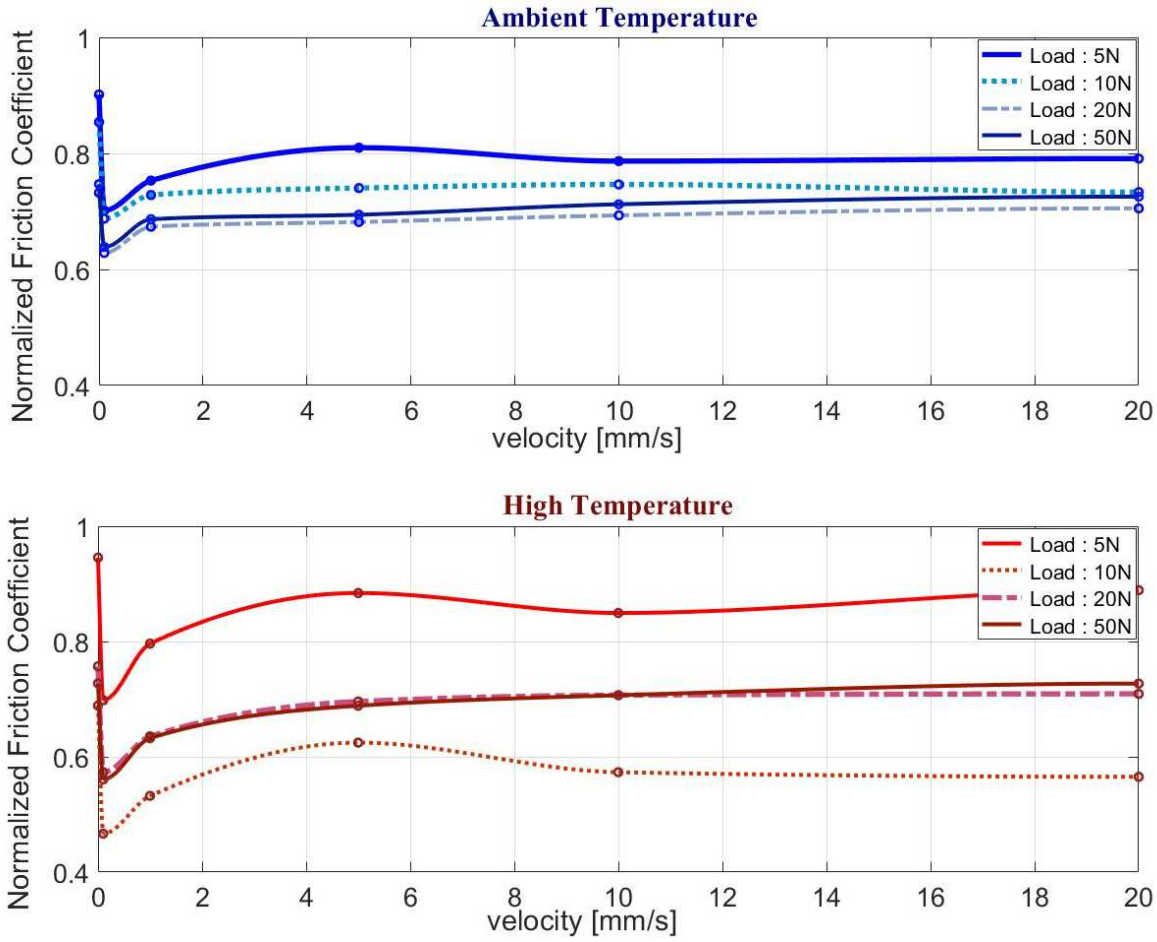

Figure 7: Normalized friction coefficient in function of the imposed sliding velocity for each tested normal load. Upper figure: tests at Ambient Temperature (27°C). Lower figure: tests at High Temperature (80°C).

From a boundary contact regime in static contact (high static friction coefficient), the role of the lubricant decreases the friction at low speed, while the interplay between the lubricant and the thickener of the grease seems to go at regime for speeds over the 10 mm/s.

The trend of the normalized friction coefficient as a function of speed is repeatable when varying the applied normal load (Figure 7). Nevertheless, for both temperature conditions, an increase in the load makes first decrease and then increase friction. Again, the increase of the contact pressure modify the response of the grease and the release of the base oil from the thickener. At high temperature this behaviour is accentuated, due to the consequent decrease in the oil viscosity and the variation of oil release from the grease.

Comparing the results obtained for the tested temperature condition, at the different normal loads, the difference between static and dynamic friction coefficient ($\mu_s - \mu_d$) is always higher at higher temperature, increasing with the increase of the applied normal load.

The tests here reported and discussed where repeated tree times for each configuration of the tested parameters. Normal loads and imposed sliding speeds have been performed in a different order to make sure that the tests order doesn't affect the results. In all the tested repeats the same behaviour of the friction coefficient was underlined and the values obtained have a dispersion of the 10% at maximum.

4. Simulation of the system dynamic response

Due to the mutual influence of the local contact conditions and the dynamical response of the system, the experimental results obtained on the frictional behaviour of the greased contact are considered as an input of a numerical lumped model of the whole mechanical system. The local frictional response is then coupled with the system dynamics by lumped numerical simulations, in order to evaluate the unstable dynamic response of the system (i.e. the stick-slip phenomena). A lumped model has been developed in order to model the whole actuator, where the brake is introduced as a slider with spring–damper system. All the main parameters of the real system are introduced into the model. This simplified model will be then used to identify the main factors of influence for the stick-slip appearance, taking into consideration both the local frictional behaviour of the bodies in contact and the system dynamic parameters.

4.1.Model description

To evaluate the dynamic response of the system, the entire actuator has been taken into account by the model (Figure 8). In Figure 1 a scheme of the whole tubular actuator is shown. An electric engine drives the loading system imposing a time varying rotational speed. The

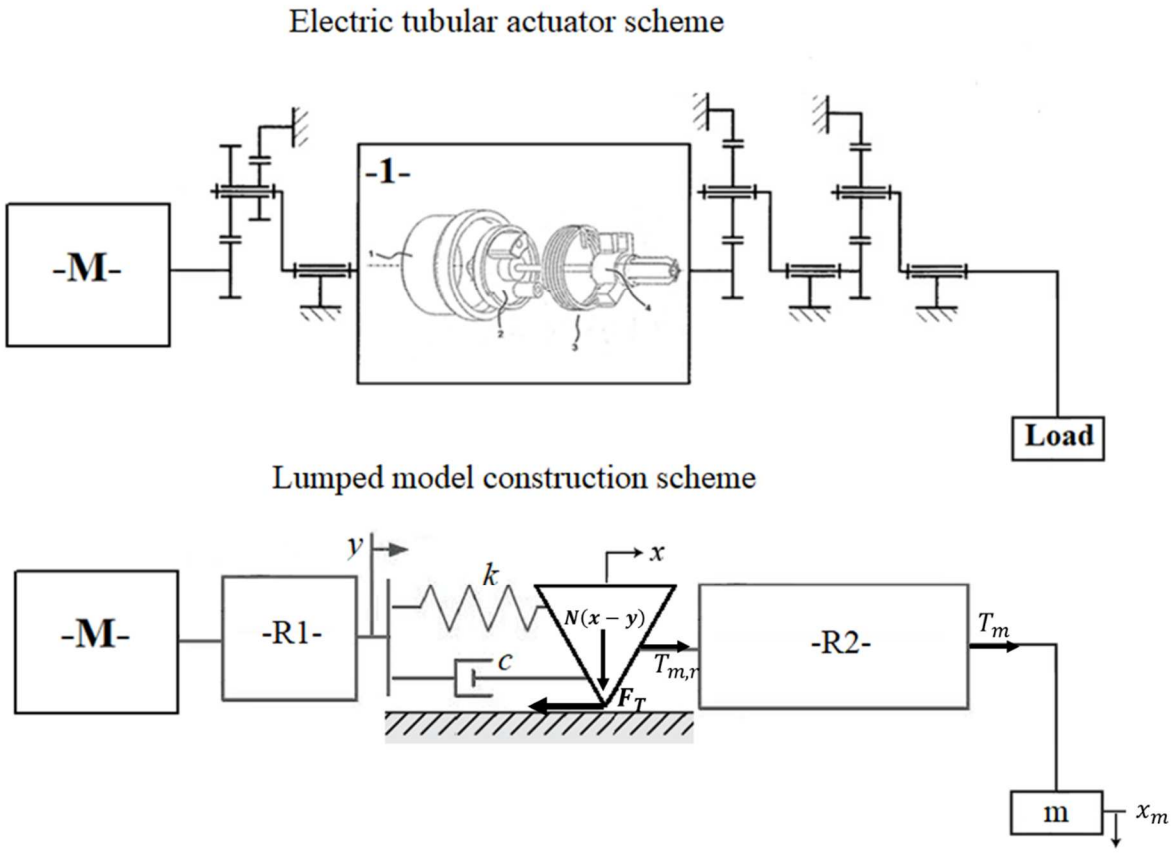

Figure 8: Tubular electric actuator operating scheme (upper figure) starting from which it was built the lumped model scheme (lower figure).

output load will be subjected to a linear speed.

A first stage of reduction R1 follows the engine and drives the spring-brake system under investigation. The brake torsional spring of the brake system is submitted to the torque

imposed by the engine by one side and the torque from the load from the other side. The torque on the torsional spring push the spring inside the drum, allowing for the braking torque. The brake is then connected to the load by a further reduction stage R2.
Starting from this scheme the lumped model has been created and the equation of motion determined. The spring-brake system is represented by a nonlinear slider-spring-damper system, where the contact load at the slider increases with the spring elongation (Figure 8 – lower figure), as occurs for the contact pressure between the torsional spring and the drum in the real brake system.
The displacement, transmitted from the engine to the brake, is reduced by the first stage of reduction (R_1) and expressed by y. On the opposite side, the force term T_m contains all the information about the output load (m) and can be written as follow:

$$T_m = mg - m\ddot{x}_m \qquad \textit{(Eq. 1)}$$

where, considering the stage of reduction:

$$\dot{x}_m = \dot{x} \cdot R_2 \qquad \textit{(Eq. 2)}$$

and

$$T_{m,r} = T_m \cdot R_2 \qquad \textit{(Eq. 3)}$$

with R_2 the reduction ratio provided by the second reduction block of the transmission (Figure 8 – R2).

Then, it is possible to write the equation of motion as follow:

$$-k(x-y) - c(\dot{x}-\dot{y}) - F_T + (-\ddot{x}m \cdot R_2 + mg) \cdot R_2 = 0 \qquad \textit{(Eq. 4)}$$

This equation takes into consideration all the key components of the tubular electric actuator under investigation.

The friction force (F_T) takes into consideration the frictional contact as follow:

$$F_T = \begin{cases} sign(\dot{x}) \cdot \mu\, N(x-y) & if F_{sum} > F_{static} Fstatic\ so\ v_r \neq 0 \\ k(x-y) + c(\dot{x}-\dot{y}) - (-\ddot{x}m \cdot R_2 + mg) \cdot R_2 & if\ v_r = 0\ and F_{sum} \leq F_{static} \end{cases} \qquad \textit{(Eq. 5)}$$

If the sum of the forces applied on the spring is higher than the static friction force and the relative speed of the spring (v_r) is different from zero, the friction force will be equal to the dynamic friction coefficient multiplied by the normal force (N) and consequently the spring is in sliding. On the contrary, if one of the two condition is not respected, the spring is in sticking on the drum.
The normal force is function of the stiffness of the spring and its elongation, imposed by the engine and load relative displacements. When the engine imposes a velocity to the axis, the torsional spring is compressed and the normal force at the greased contact will decrease, decreasing the brake torque until the rotation of the spring and the descent of the load.

In the present model the coefficient of friction is not assumed to be a constant value (Coulomb-Amounts friction law). The experimental frictional analysis, performed on the

Triboair test bench (Section 3), shows that the macroscopic friction coefficient undergoes relevant variations as a function of imposed boundary conditions. Based on the results from the experimental frictional analysis, a more realistic friction model has been implemented in the model. The friction coefficient values are the curves obtained experimentally, as a function of the sliding velocity.

The described lumped model allows to analyse the conditions under which the contact stick-slip instability can occur by analysing the dynamic response of the entire system as a function of the local frictional response of the lubricated contact.

4.2.System response under greased frictional contact

The numerical lumped model has been developed and alimented by the data from the frictional tests, in order to recreate the scenario that brings to the frictional instability. The reduction ratios and efficiency factors of the reduction stages, together with the imposed velocity of the real actuator are introduced as inputs of the lumped model. The equation of motion has been then solved by a Simulink code and the outputs of the model are analysed.
Figure 9 presents the results obtained, introducing the friction coefficient, previously obtained thought the experimental tests, at ambient and high temperature.
The velocity curve imposed by the engine, starts from 0 and reaches the maximum speed of 0.5 m/s within 1 second. The imposed velocity is kept stable for 18 seconds and subsequently reset to zero by a deceleration ramp lasting 1 second.
The same trend of the imposed velocity has been set both for the ambient and the high temperature simulations (Figure 9 - A); the only difference is in the different friction coefficient behaviours introduced as an input.

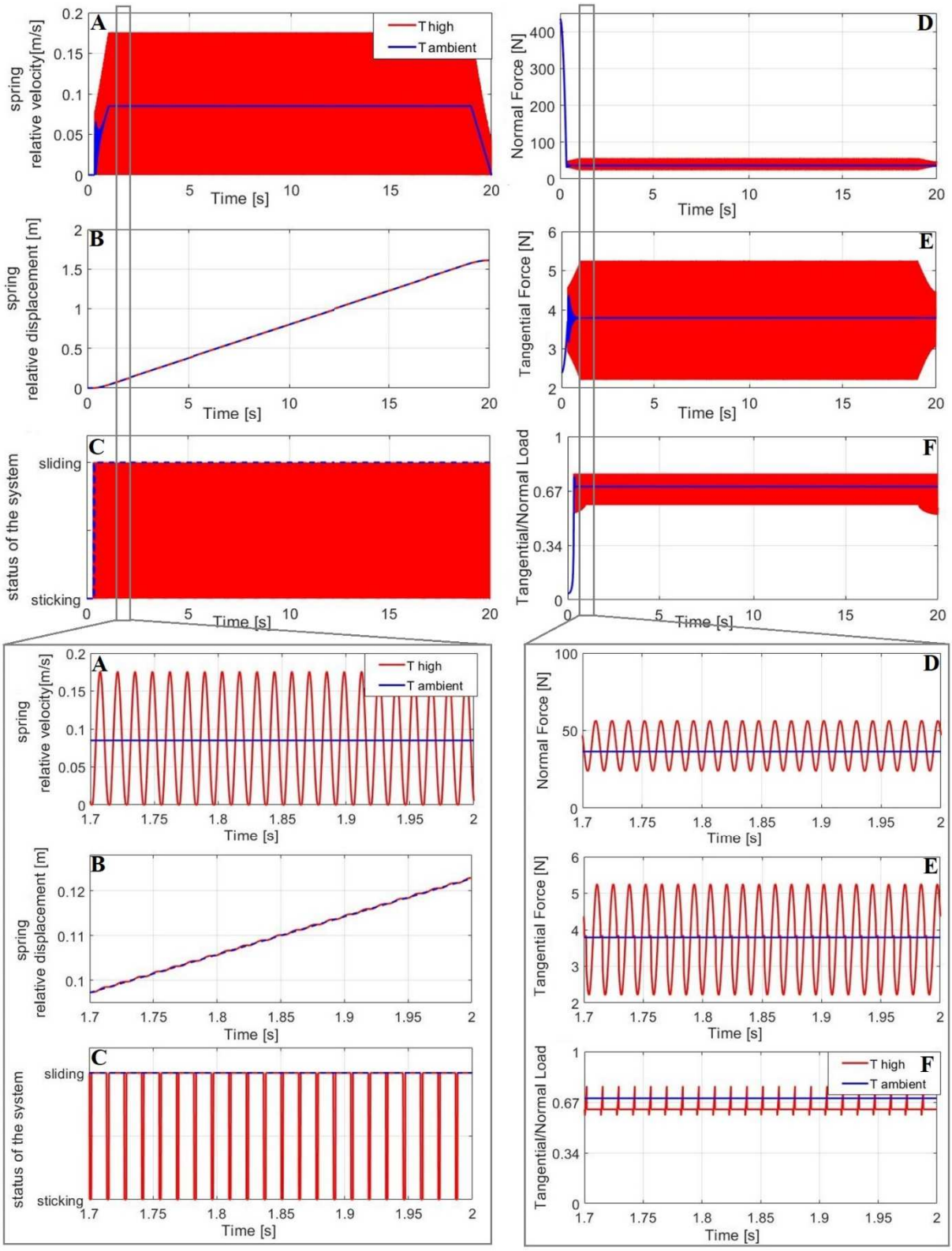

Figure 9: Numerical simulations result of the tested conditions both at Ambient and High Temperature. Down: zoom of the curves in the time interval of [1.7 - 2 seconds].

Considering the case of the ambient temperature conditions, (Figure 9 - blue curves), after some seconds the spring starts sliding and the velocity starts to increase according to the imposed conditions. The normal force (Figure 9 - D) decreases due to the elongation of the

spring, reaching the equilibrium. A small initial oscillation can be noticed just after the displacement starts, due to the imposed characteristics of stiffness and damping of the system. In this case, contact instability does not occur as can be seen looking at the status of the system, which is in continuous sliding (Figure 9 - C, blue curve).
On the contrary, analysing the same situation in the case of high temperature conditions (Figure 9 - red curves), maintaining all the same operating conditions, it is possible observe the occurrence of the stick-slip instability. The contact status shift periodically between sticking and sliding (Figure 9 - C, red curve). The speed (Figure 9 - A, red curve) oscillates between zero, during the stick phases, and a maximum value due to the system oscillation. The spring displacement is represented by the classic jerking motion, with a step-wise curve (Figure 9 - B, red curve). The normal force oscillates around the equilibrium value (Figure 9 - D, red curve), due to the periodic oscillation of the spring elongation during the instability. Consequently, the tangential force (Figure 9 - E, red curve) follows the normal load oscillation during the sliding phases, while it increases during the sticking phases until shifting again in sliding. Analyzing the ratio between normal and tangential force (Figure 9 - F, red curve), the characteristic shift between static and dynamic friction are recognized, passing from sticking to sliding conditions.
Figure 10 shows the comparison between the lumped model results and the actuator behavior during frictional instability.

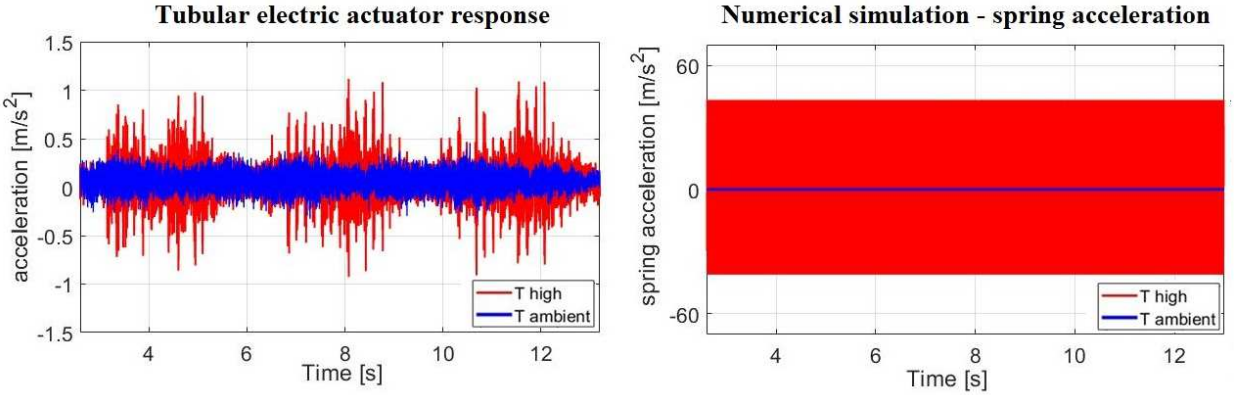

Figure 10: Comparison between the acceleration over the time recovered from the actuator (left side) and the velocity over the time obtained with the lumped model (right side), both for ambient (blue curve) and high (red curves) temperature.

The effect of the different frictional response of the greased with respect temperature is highlighted. The results of the lumped model show a strong correlation with the dynamic response of the actuator, in terms of acceleration over the time, both for ambient (Figure 10 - blue curves) and high (Figure 10 - red curves) temperature conditions. The increase in the friction-velocity slope (difference between static and dynamic friction coefficient) recovered experimentally (Figure 6), and implemented into the lumped model, is at the origin of the frictional stick-slip instability.

5. Conclusions

Lubricated systems are supposed to reduce the frictional losses, but they can also collaborate in the appearance of dynamic contact instability, due to the friction-velocity characteristics when passing from boundary to mixed contact regimes. Understanding the conditions for which the system is more predisposed to the stick-slip phenomenon may allow for preventing the appearance of such instabilities. In the present work, an approach to the stick-slip problem of a greased contact, applied to a real case study, is proposed.

An experimental campaign has been first developed for the characterization of the frictional response of the greased contact, analyzing the local behavior in terms of friction coefficient at different speeds, pressures and temperatures.

The main outcomes from the experimental campaign can be summarized as follow:

- After a higher static friction coefficient (μ_s), the friction coefficient curve, as a function of the sliding velocity, drops rapidly until a lower dynamic coefficient (μ_d) is reached; then it increases again and stabilizes at higher speed. This trend of the friction coefficient is independent from the temperature and the applied normal load.
- The values of the friction first decrease and then increase with the applied load.
- The difference between μ_s and μ_d is higher in the case of high temperature conditions and it decrease increasing the applied normal load.

These characteristic trend of the frictional response can be attributed to the competition between the oil and thickener contribution in the overall response of grease, as a function of temperature and contact pressure.

Then, a numerical lumped model of the actuator has been developed and alimented by the data from both the real mechanical system and the experimental frictional tests. When introducing the different frictional responses recovered experimentally at high and ambient temperature, the results from the numerical simulations show stick-slip at higher temperature and stable sliding response at ambient temperature, as observed experimentally on the real system. These results allow for asserting that the friction-velocity response of the greased contact is the key parameter that destabilize the system, bringing to the stick-slip instability. Once validated the model, further parametrical simulations will be addressed for identifying the role of the mechanical parameters of the system on the stick-slip occurrence.

REFERENCES

[1] D. Tonazzi, F. Massi, L. Baillet, A. Culla, M. Di Bartolomeo, and Y. Berthier, 'Experimental and numerical analysis of frictional contact scenarios: from macro stick–slip to continuous sliding', *Meccanica*, vol. 50, no. 3, pp. 649–664, Mar. 2015.

[2] F. Massi, A. Saulot, M. Renouf, and G. Messager, 'Simulation of dynamic instabilities induced by sliding contacts', in *DINAME 2013*, Brazil, 2013, p. Cd-Rom 9p.

[3] C. Gao, D. Kuhlmann-Wilsdorf, and D. D. Makel, 'Fundamentals of stick-slip', *Wear*, vol. 162–164, pp. 1139–1149, Apr. 1993.

[4] A. Meziane, L. Baillet, and B. Laulagnet, 'Experimental and numerical investigation of friction-induced vibration of a beam-on-beam in contact with friction', *Applied Acoustics*, vol. 71, no. 9, pp. 843–853, 2010.

[5] J. B. Sampson, F. Morgan, D. W. Reed, and M. Muskat, 'Studies in Lubrication: XII. Friction Behavior During the Slip Portion of the Stick-Slip Process', *Journal of Applied Physics*, vol. 14, no. 12, pp. 689–700, Dec. 1943.

[6] D. Tonazzi *et al.*, 'Numerical analysis of contact stress and strain distributions for greased and ungreased high loaded oscillating bearings', *Wear*, vol. 376–377, pp. 1164–1175, 2017.

[7] I. Ghezzi *et al.*, 'Damage evolution and contact surfaces analysis of high-loaded oscillating hybrid bearings', *Wear*, vol. 406–407, pp. 1–12, Jul. 2018.

[8] Y. Waddad, V. Magnier, P. Dufrénoy, and G. De Saxcé, 'Multiscale thermomechanical modeling of frictional contact problems considering wear – Application to a pin-on-disc system', *Wear*, vol. 426–427, pp. 1399–1409, Apr. 2019.

[9] A. Meziane, B. Bou-Saïd, and J. Tichy, 'Modelling human hip joint lubrication subject to walking cycle', *Lubrication Science*, vol. 20, no. 3, pp. 205–222, 2008.

[10] J.-J. Sinou, J. Cayer-Barrioz, and H. Berro, 'Friction-induced vibration of a lubricated mechanical system', *Tribology International*, vol. 61, pp. 156–168, May 2013.

[11] J. Zuleeg, 'Controlling Stick-Slip Noise Generation with Lubricants'.

[12] B. Bhushan, 'Stick-Slip Induced Noise Generation in Water-Lubricated Compliant Rubber Bearings', *J. of Lubrication Tech*, vol. 102, no. 2, pp. 201–210, Apr. 1980.

[13] F. Dalzin, A. Le Bot, J. Perret-Liaudet, and D. Mazuyer, 'Tribological origin of squeal noise in lubricated elastomer–glass contact', *Journal of Sound and Vibration*, vol. 372, pp. 211–222, Jun. 2016.

[14] S. Andersson, A. Söderberg, and S. Björklund, 'Friction models for sliding dry, boundary and mixed lubricated contacts', *Tribology International*, vol. 40, no. 4, pp. 580–587, Apr. 2007.

[15] I. Ghezzi *et al.*, 'Examination of stick-slip scenario on lubricated spring-brake systems', presented at the Proceedings of the LACCEI international Multi-conference for Engineering, Education and Technology, 2019, vol. 2019-July.

[16] R. A. Ibrahim, 'Friction-Induced Vibration, Chatter, Squeal, and Chaos—Part I: Mechanics of Contact and Friction', *Appl. Mech. Rev*, vol. 47, no. 7, pp. 209–226, Jul. 1994.

[17] D. Tonazzi *et al.*, 'Experimental and numerical characterization of system response under dry frictional contact', Sep. 2014.

[18] T. Eray, B. Sümer, and İ. Murat Koç, 'Analytical and experimental analysis on frictional dynamics of a single elastomeric pillar', *Tribology International*, vol. 100, pp. 293–305, Aug. 2016.

[19] J.-J. Sinou, F. Thouverez, and L. Jezequel, 'Analysis of friction and instability by the centre manifold theory for a non-linear sprag-slip model', *Journal of Sound and Vibration*, vol. 265, no. 3, pp. 527–559, Aug. 2003.

[20] N. Hoffmann and L. Gaul, 'A sufficient criterion for the onset of sprag-slip oscillations', *Archive of Applied Mechanics*, vol. 73, no. 9, pp. 650–660, Apr. 2004.

[21] K. Bonnay, V. Magnier, J. F. Brunel, P. Dufrénoy, and G. De Saxcé, 'Influence of geometry imperfections on squeal noise linked to mode lock-in', *International Journal of Solids and Structures*, vol. 75–76, pp. 99–108, Dec. 2015.

[22] F. Cantone and F. Massi, 'A numerical investigation into the squeal instability: Effect of damping', *Mechanical Systems and Signal Processing*, vol. 25, no. 5, pp. 1727–1737, Jul. 2011.

[23] A. Lazzari, D. Tonazzi, G. Conidi, C. Malmassari, A. Cerutti, and F. Massi, 'Experimental Evaluation of Brake Pad Material Propensity to Stick-Slip and Groan Noise Emission', *Lubricants*, vol. 6, no. 4, p. 107, Dec. 2018.

[24] J. Awrejcewicz and P. Olejnik, 'Analysis of Dynamic Systems With Various Friction Laws', *Applied Mechanics Reviews*, vol. 58, no. 6, p. 389, 2005.

[25] E. Berger, 'Friction modeling for dynamic system simulation', *Applied Mechanics Reviews*, vol. 55, no. 6, p. 535, 2002.

[26] J. Abdo and A. Ali, 'Analytical approach to estimate amplitude of stick-slip oscillations', *Journal of Theoretical and Applied Mechanics*, vol. 49, Jan. 2011.

[27] J. H. Dieterich, 'Time-Dependent Friction and the Mechanics of Stick-Slip', in *Rock Friction and Earthquake Prediction*, J. D. Byerlee and M. Wyss, Eds. Basel: Birkhäuser Basel, 1978, pp. 790–806.

[28] D. Tonazzi, F. Massi, A. Culla, L. Baillet, A. Fregolent, and Y. Berthier, 'Instability scenarios between elastic media under frictional contact', *Mechanical Systems and Signal Processing*, vol. 40, no. 2, pp. 754–766, Nov. 2013.

[29] G. Lacerra, M. Di Bartolomeo, S. Milana, L. Baillet, E. Chatelet, and F. Massi, 'Validation of a new frictional law for simulating friction-induced vibrations of rough surfaces', *Tribology International*, vol. 121, pp. 468–480, May 2018.

[30] M. Di Bartolomeo, F. Massi, L. Baillet, A. Culla, A. Fregolent, and Y. Berthier, 'Wave and rupture propagation at frictional bimaterial sliding interfaces: From local to global

dynamics, from stick-slip to continuous sliding', *Tribology International*, vol. 52, pp. 117–131, Aug. 2012.

[31] Y. Ben-Zion, 'Dynamic ruptures in recent models of earthquake faults', *Journal of the Mechanics and Physics of Solids*, vol. 49, no. 9, pp. 2209–2244, Sep. 2001.

[32] G. G. Adams, 'Self-Excited Oscillations of Two Elastic Half-Spaces Sliding With a Constant Coefficient of Friction', *Journal of Applied Mechanics*, vol. 62, no. 4, pp. 867–872, Dec. 1995.

[33] D. Tonazzi, F. Massi, L. Baillet, J. Brunetti, and Y. Berthier, 'Interaction between contact behaviour and vibrational response for dry contact system', *Mechanical Systems and Signal Processing*, vol. 110, pp. 110–121, Sep. 2018.

[34] S. S. Antoniou, A. Cameron, and C. R. Gentle, 'The friction-speed relation from stick-slip data', *Wear*, vol. 36, no. 2, pp. 235–254, Feb. 1976.

[35] Li Chun Bo and D. Pavelescu, 'The friction-speed relation and its influence on the critical velocity of stick-slip motion', *Wear*, vol. 82, no. 3, pp. 277–289, Nov. 1982.

[36] İ. M. Koç and C. Aksu, 'Tactile sensing of constructional differences in fabrics with a polymeric finger tip', *Tribology International*, vol. 59, pp. 339–349, Mar. 2013.

[37] D. Tonazzi, F. Massi, M. Salipante, L. Baillet, and Y. Berthier, 'Estimation of the Normal Contact Stiffness for Frictional Interface in Sticking and Sliding Conditions', *Lubricants*, vol. 7, no. 7, p. 56, Jul. 2019.

[38] A. Lazzari, D. Tonazzi, and F. Massi, 'Squeal propensity characterization of brake lining materials through friction noise measurements', *Mechanical Systems and Signal Processing*, vol. 128, pp. 216–228, Aug. 2019.

[39] D. Tonazzi, F. Massi, A. Culla, A. Fregolent, and Y. Berthier, 'Role of damping on contact instability scenarios', in *5° World Tribology Congress*, Turin, Italy, 2013.

[40] I. Serrano-Munoz, J. Rapontchombo, V. Magnier, F. Brunel, S. Kossman, and P. Dufrénoy, 'Evolution in microstructure and compression behaviour of a metallic sintered friction material after braking', *Wear*, vol. 436–437, 2019.

[41] B. Jacobson, 'The Stribeck memorial lecture', *Tribology International*, vol. 36, no. 11, pp. 781–789, Nov. 2003.

[42] B. Armstrong-Helouvry, 'Stick-slip arising from Stribeck friction', in *, IEEE International Conference on Robotics and Automation Proceedings*, 1990, pp. 1377–1382 vol.2.

[43] A. Tranchand, 'Actionneur électromécanique, installation de fermeture ou de protection solaire comprenant un tel actionneur et procédé de contrôle d'un tel actionneur', EP2746526A1, 25-Jun-2014.

[44] E. Lagarde and F. Negrello, 'Spring brake for the actuator of a screen for a building and actuator equipped with such brake', EP2230415A1, 22-Sep-2010.

[45] E. Lagarde and D. Menetrier, 'Actionneur électrique d'entraînement d'un écran domotique', EP2267330A1, 29-Dec-2010.

[46] M. Stender, M. Di Bartolomeo, F. Massi, and N. Hoffmann, 'Revealing transitions in friction-excited vibrations by nonlinear time-series analysis', *Nonlinear Dyn*, May 2019.